NEGATIVE BINOMIAL PROPERTIES AND CLAN STRUCTURE IN MULTIPLICITY DISTRIBUTIONS*

By A. Giovannini** and L. Van Hove

CERN, Geneva, Switzerland

(Received December 3, 1987)

We review the negative binomial properties measured recently for many multiplicity distributions of high energy hadronic, semi-leptonic and leptonic reactions in selected rapidity intervals. We analyse them in terms of the "clan" structure which can be defined for any negative binomial distribution. By comparing reactions we exhibit a number of regularities for the average number $\bar{N}$ of clans and the average charged multiplicity $\bar{n}_c$ per clan.

PACS numbers: 13.85.–t, 13.65.+i, 13.60.H, 12.40.A

1. Introduction

The study of multiplicity distributions (MDs) in high energy hadronic, leptonic and semileptonic processes has revealed an unsuspected and striking phenomenon: charged particle MDs have a negative binomial (NB) shape over a wide energy range in full phase space and in symmetric rapidity windows $|y| < y_0$ (y = longitudinal rapidity in the c.m. frame).

The main experiments have been so far:

— UA5 Collaboration at SPS $p\bar{p}$ Collider, c.m. energies $\sqrt{s}$ = 200 GeV, 540 GeV, 900 GeV (here for the window analysis, the pseudorapidity variable is used instead of the rapidity) [1].

— HRS Collaboration at PEP, e^+e^- annihilation, $\sqrt{s}$ = 29 GeV (the longitudinal direction is defined by the thrust axis of the final state particles) [2].

— NA22 Collaboration with the European Hybrid Spectrometer, pp and π^+p collisions at $\sqrt{s}$ = 22 GeV (the pp and π^+p data are very close to each other; here the NB regularity was also found for negative particles and in π^+p for the forward and backward hemispheres taken separately) [3].

---

* Expanded and updated version of a lecture presented by A. Giovannini at the XXVII Cracow School of Theoretical Physics, Zakopane, Poland, June 3–15, 1987.

** On leave of absence from Dipartimento di Fisica Teorica, Universitá di Torino and INFN, Sezione di Torino. Supported in part by Ministero della Pubblica Istruzione (Italy) under Grant 1986.

— European Muon Collaboration (EMC), deep inelastic muon-proton scattering in eight intervals of the total c.m. energy of the hadronic system, W, from $W = 4 \div 6$ GeV to $W = 18 \div 20$ GeV (here the regularity was also found in the forward and backward hemispheres taken separately) [4].
— NA5 Experiment, proton-proton, proton-Xenon and proton-Argon collisions at $p_{lab} = 200$ GeV/c (here the NB regularity occurs separately in the forward and backward hemispheres for charged and for negative particles, and in symmetric windows for negatives; for charged particles it fails in large symmetric windows) [5].
— New results, still preliminary, on MDs in rapidity intervals at the ISR have been presented. They seem to follow the same general NB trend [6].

In the μp experiments [4], departures from NB behaviour are seen below $W \simeq 10$ GeV for total charged multiplicities. The distributions become narrower with Poisson shape or positive, i.e., ordinary binomial shape. However, the NB behaviour is preserved in central rapidity intervals. The origin of this effect is presumably due to energy-momentum conservation which strongly affects the fragmentation regions, and at low W these contribute a major fraction of the total multiplicity.

The challenging question is to interpret the wide occurrence of the NB regularity in terms of a general mechanism common to hadronic, leptonic and semileptonic processes. We have argued [7] that the most likely explanation is some form of cascading (or shower) mechanism of particle production, and we have introduced the term "clan" for groups of particles of common ancestry in such a cascade (for convenience, we define clans to contain at least one charged particle). By a well-known mathematical property of the NB distribution (see the Appendix), one can assume the clans to be produced independently (Poisson distribution for the number N of clans); if the MD of an average clan is logarithmic, the overall MD is then NB. The parameters which characterize the clan structure are the average number of clans, $\bar{N}$, and the average number of charged particles per clan, $\bar{n}_c$. As shown in the Appendix, they are linked to the usual parameters $\bar{n}$ and k of the NB distribution by

$$\bar{N} = \bar{n}/\bar{n}_c = k \ln\left(1 + \frac{\bar{n}}{k}\right).$$

Note that $\bar{n}_c$ depends only on the ratio $\bar{n}/k$ and is always > 1, with $\bar{n}_c = 1$ for a Poisson distribution ($k = \infty$).

In Section 2 we briefly review the main properties of the experimental NB distributions presented in Refs. [1–3] by analysing their clan structure for symmetric rapidity windows $|y| < y_0$. Then we compare the results with those emerging from a similar analysis of the EMC experiment [4]. This comparison is possible because the highest EMC hadronic energy ($W = 18 \div 20$ GeV) is close to the energy $\sqrt{s} = 22$ GeV of the NA22 experiment on π^+p and pp [3].

Section 3 is devoted to the discussion of MDs in forward and backward rapidity windows, $0 < y < y_0$ and $-y_0 < y < 0$ respectively, and also in "moving rapidity windows", i.e., intervals $|y - y_1| < y_0$ with fixed $y_0 = 0.5$ and variable y_1. In Section 4 we review the NB behaviour observed in proton-nucleus collisions and mention some related

theoretical work. Section 5 discusses Kittel's recent "Monte Carlo e^+e^- annihilation experiments" at $\sqrt{s} = 29$, 200 and 2000 GeV. We also mention further work on the same topic, which led us to a simple physical picture for the clan structure at partonic level and for the relation between partonic and hadronic MDs. We present a summary and concluding remarks in Section 6, and the Appendix mentions the relevant mathematical properties of NB distributions.

2. *Clan structure in hadronic, leptonic and semi-leptonic processes — symmetric rapidity windows*

Figure 1 shows the most remarkable result of the clan analysis: in *hadronic collisions* the average number $\bar{N}$ of clans for fixed rapidity windows is approximately energy-independent over the large energy range $\sqrt{s} = 22$–900 GeV. While this result is not yet understood theoretically, it is very striking and justifies in our view the use of the clan analysis to describe the NB properties. As we shall see, it also holds for the μp data and for the parton shower model predictions of e^+e^- annihilation.

The main properties of the average charged multiplicity $\bar{n}_c$ per clan, shown in Fig. 1b, are the following:

a) $\bar{n}_c$ increases rapidly with energy; since $\bar{N}$ is almost constant the overall growth of multiplicity is due to this increase of clan size,

b) $\bar{n}_c$ is becoming larger as the rapidity window increases, reaching a maximum and then eventually decreasing (this decrease is clearly visible in pp and π^+p at $\sqrt{s} = 22$ GeV, but is at most very weak in $p\bar{p}$ at $\sqrt{s} = 200$–900 GeV).

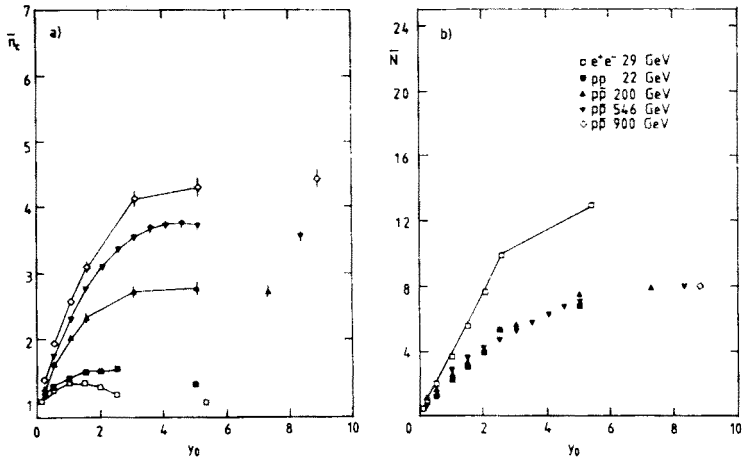

Fig. 1. a) Average charged multiplicity $\bar{n}_c$ per clan and b) average number of clans $\bar{N}$, as a function of the size of a symmetric rapidity window $|y| < y_0$ for the collisions and energies indicated. For $p\bar{p}$ data y is the pseudo-rapidity. The points at the highest y_0 value correspond to the respective phase space limits $y_{max} = \ln(\sqrt{s}/m_\pi)$. This figure is adapted from Fig. 1 of Ref. [16]. The π^+p data at 22 GeV (not plotted here) are very close to the pp data. They are plotted in Figs. 2 and 3

The e^+e^- *annihilation* data at $\sqrt{s} = 29$ GeV, also shown in Fig. 1, give values of $\bar{N}$ and $\bar{n}_c$ which are very different from those of pp and π^+p at the comparable c.m. energy $\sqrt{s} = 22$ GeV. The e^+e^- annihilation clans are more numerous than in hh collisions (larger $\bar{N}$), but their multiplicity is smaller (smaller $\bar{n}_c$).

We now compare these results with the new data of the EMC for *muon proton deep inelastic scattering*, selecting the c.m. energy intervals $W = 6 \div 8$ GeV and $W = 18 \div 20$ GeV. Figures 2 and 3 give the values of $\bar{N}$ and $\bar{n}_c$ in symmetric rapidity windows $|y| < y_0$ and in windows $0 < \pm y < y_0$ of the forward and backward c.m. hemispheres of the hadronic system[1]. The W intervals have been selected in order to compare the behaviour of clan parameters at low energy with the highest W available for semi-leptonic collisions. The parameters at intermediate energies W vary smoothly between the above two. In Figs. 2 and 3 we have also plotted the parameters $\bar{N}$ and $\bar{n}_c$ for π^+p at $\sqrt{s} = 22$ GeV and for e^+e^- at $\sqrt{s} = 29$ GeV (the latter already appear in Fig. 1).

The present Section analyses the clan structure in symmetric rapidity windows [curves (S) in Figs. 2 and 3]. In Fig. 2 one sees that $\bar{N}$ is essentially constant for $y_0 \lesssim 1$ although W increases from $6 \div 8$ to $18 \div 20$ GeV. A variation appears for larger y_0; it is at $y_0 \simeq 1.5$ that the $6 \div 8$ distribution goes over from a NB to a positive binomial (for which an interpretation in terms of clans makes no sense, see Appendix). At $18 \div 20$ GeV the values

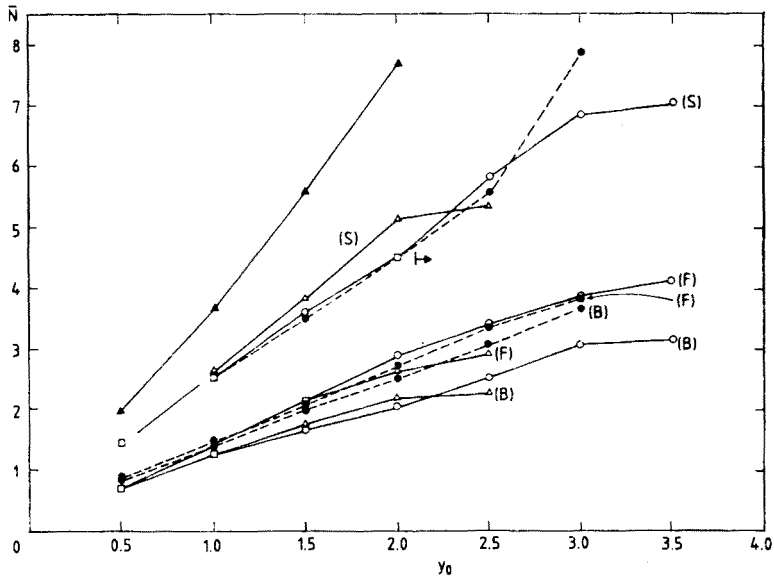

Fig. 2. Average number of clans, $\bar{N}$, in the following experiments: ▲—▲ e^+e^- ($\sqrt{s} = 29$ GeV), ●---● π^+p ($\sqrt{s} = 22$ GeV), △—△ μp ($W = 6 \div 8$ GeV), ○—○ μp ($W = 18 \div 20$ GeV), in rapidity windows $|y| < y_0$ (S), $0 < y < y_0$ (F) and $-y_0 < y < 0$ (B). The symbol □ indicates the overlap of two points, and → indicates the limit above which the π^+p data are taken for even multiplicities only

[1] The forward hemisphere, $y > 0$, is defined for μp collisions as corresponding to the fragmentation region of the "current quark" struck by the virtual photon. For π^+p it corresponds to the pion hemisphere. The windows $0 < \pm y < y_0$ are discussed in Section 3.

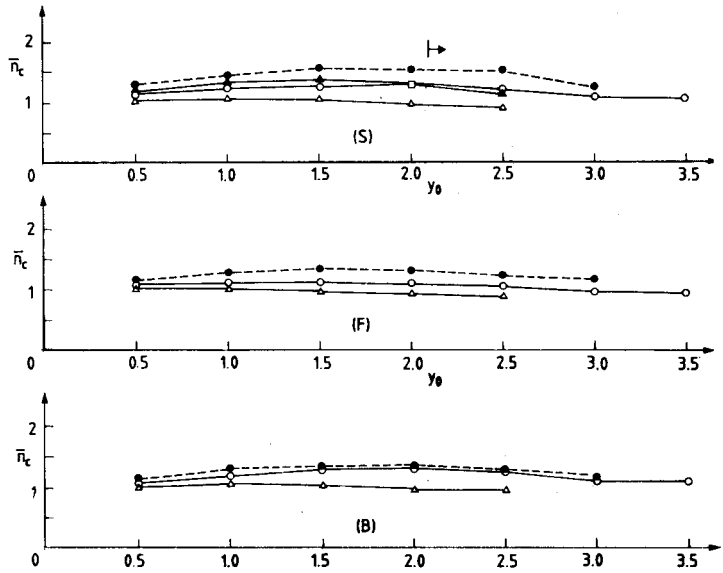

Fig. 3. Average charged multiplicity per clan, $\bar{n}_c$. Same notation as in Fig. 2, but the values for $|y| < y_0$ (S), $0 < y < y_0$ (F) and $-y_0 < y < 0$ (B) are plotted separately

of $\bar{N}$ for $y_0 \lesssim 2$ are very close to those of π^+p at $\sqrt{s} = 22$ GeV (the values of π^+p for $y_0 > 2$ refer to even multiplicities only), and they lie far below the corresponding $\bar{N}$ values for e^+e^- annihilation at $\sqrt{s} = 29$ GeV.

As shown in Fig. 3 (S), for fixed y_0 the average number $\bar{n}_c$ of particles per clan increases significantly with W. For fixed W it first increases with y_0 and then decreases. For $18 \div 20$ GeV, it reaches a maximum of ~ 1.5 at $y_0 \sim 2$. At $6 \div 8$ GeV, its maximum is ~ 1.08 reached at $y_0 \sim 1$, and $\bar{n}_c$ becomes < 1 for $y_0 \gtrsim 1.5$ (positive binomial). For $W = 18 \div 20$ GeV, $\bar{n}_c$ has approximately the same values as in e^+e^- annihilation at $\sqrt{s} = 29$ GeV, but is significantly below the corresponding values in π^+p at $\sqrt{s} = 22$ GeV. Interestingly, this is the opposite of what occurs for $\bar{N}$. It therefore appears that for μp in symmetric windows the behaviour of the number of clans tends to have hadronic character while that of the clan size tends to be leptonic. The analysis of these trends will be refined in the next Section.

3. Forward versus backward hemispheres and moving rapidity windows

We now discuss the μp results in the forward and backward hemispheres (FH and BH respectively). They are given in Figs. 2 and 3 by the curves marked (F) and (B). Contrary to what happens for π^+p, we notice a sizeable difference between the clan structures of μp in the two hemispheres, i.e., between the quark and diquark fragmentation regions: clans are more numerous but smaller in size in FH than BH. In both hemispheres $\bar{N}$ is approximately energy independent for $y_0 \lesssim 1.5$, more so than for symmetric windows. In contrast, $\bar{n}_c$ grows appreciably with W in both hemispheres, especially in BH, as illustrat-

ed by the values of the maxima [FH: $(\bar{n}_c)_{max} \simeq 1.03$ at $y_0 \simeq 1$ for $W = 6 \div 8$ GeV and $(\bar{n}_c)_{max} \simeq 1.13$ at $y_0 \simeq 1.5$ for $W = 18 \div 20$ GeV; to be compared with BH: $(\bar{n}_c)_{max} \simeq 1.07$ at $y_0 \simeq 1$ for $W = 6 \div 8$ GeV and $(\bar{n}_c)_{max} \simeq 1.3$ at $y_0 \simeq 2$ for $W = 18 \div 20$ GeV].

The parameter $\bar{N}$ for μp is quite close to the π^+p values in FH, while it is smaller in BH. Again things tend to be opposite for $\bar{n}_c$; at $W = 18 \div 20$ GeV, it is close to π^+p in BH but is smaller in FH where it is presumably close to e^+e^- values or even somewhat smaller (we do not have e^+e^- MDs for single hemispheres). At the end of Section 2, we remarked for symmetric windows that the behaviour of $\bar{N}$ tends to be hadronic whereas that of $\bar{n}_c$ tends to be leptonic. We now see that the hadronic behaviour of $\bar{N}$ and probably also the leptonic behaviour of $\bar{n}_c$ are concentrated mainly in FH, i.e., in the current quark fragmentation region. In BH (diquark fragmentation) the clan size ($\bar{n}_c$) is larger than leptonic and close to hadronic, whereas the number of clans ($\bar{N}$) is smaller than hadronic (and surely much smaller than leptonic). These remarkable trends will be confirmed below in our discussion of moving rapidity windows. Taken together with the energy independence of $\bar{N}$ for fixed windows, they support our view that the clan structure analysis is more than a mathematical parametrization of the data and must have dynamical relevance.

We now discuss the clan structure of hadronic and semi-leptonic reactions in rapidity windows of unit size, $|y - y_1| < 0.5$, with the centre y_1 moving from -3 to 3. To this effect we plot in Fig. 4 the clan parameters $\bar{N}$, $\bar{n}_c$ for $p\bar{p}$ at $\sqrt{s} = 540$ GeV [8], π^+p at $\sqrt{s} = 22$ GeV [9] and μp at $W = 6 \div 8$ GeV, $W = 18 \div 20$ GeV [10].

For $p\bar{p}$ at 540 GeV the average number of clans is approximately constant ($\bar{N} \simeq 1.8$) in $-3 < y_1 < 3$ with a shallow dip in the centre. A similar behaviour is found at $\sqrt{s} = 22$ GeV in $-2 < y_1 < 2$ for π^+p ($\bar{N} \simeq 1.4$ in BH, $\bar{N} \simeq 1.5$ in FH) and also for pp ($\bar{N} \simeq 1.4$, data from Ref. [9], not plotted), with a decrease at larger $|y_1|$. The behaviour of $\bar{N}$ is different for μp, where the data show a sizeable asymmetry between FH and BH. At $W = 18 \div 20$ GeV, $\bar{N}$ in FH has values close to those of π^+p ($\bar{N} \simeq 1.5$ up to $y_1 \simeq 2$,

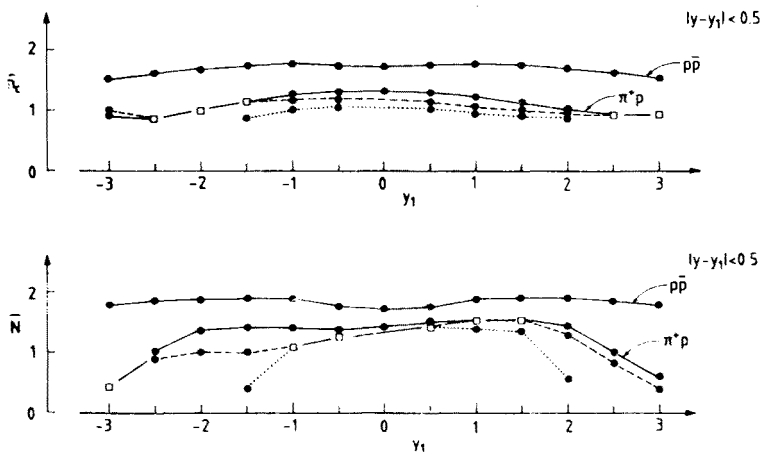

Fig. 4. $\bar{N}$ and $\bar{n}_c$ in rapidity windows $|y - y_1| < 0.5$ with centre y_1 moving along the rapidity axis. ●—● π^+p ($\sqrt{s} = 22$ GeV) and $p\bar{p}$ ($\sqrt{s} = 540$ GeV) as indicated in the figure, ●---● μp ($W = 18 \div 20$ GeV), ●····● μp ($W = 6 \div 8$ GeV). The symbol □ indicates the overlap of points

TABLE

Test of the additivity relation (A.27) of the Appendix for the μp reaction at $W = 18 \div 20$ GeV

	$\bar{n}$	k^{-1}	$\bar{n}/k$	
D_1: $-0.5 < y < 0$	0.77 ± 0.01	0.209 ± 0.039	0.161 ± 0.028	SUM
D_2: $-1.5 < y < -0.5$	1.33 ± 0.01	0.309 ± 0.021	0.411 ± 0.031	0.572 ± 0.042
D: $-1.5 < y < 0$	2.13 ± 0.03	0.268 ± 0.017	0.571 ± 0.044	
D_1: $0 < y < 0.5$	0.79 ± 0.01	0.215 ± 0.017	0.170 ± 0.016	SUM
D_2: $0.5 < y < 1.5$	1.61 ± 0.01	0.087 ± 0.011	0.140 ± 0.010	0.310 ± 0.019
D: $0 < y < 1.5$	2.43 ± 0.01	0.113 ± 0.006	0.275 ± 0.016	
D_1: $\lvert y \rvert < 0.5$	1.57 ± 0.02	0.212 ± 0.014	0.333 ± 0.026	
D_2: $0.5 < y < 1.5$	1.61 ± 0.01	0.087 ± 0.011	0.140 ± 0.010	SUM
D_3: $-1.5 < y < -0.5$	1.33 ± 0.01	0.309 ± 0.021	0.411 ± 0.031	0.884 ± 0.042
D: $\lvert y \rvert < 1.5$	4.56 ± 0.03	0.127 ± 0.005	0.579 ± 0.027	

then quickly decreasing), while in BH the $\bar{N}$ of μp falls well below the π^+p values, confirming the trend noted in the analysis of the windows $0 < \pm y < y_0$. Regarding the energy dependence of the μp data, one finds the usual property that $\bar{N}$ depends very little on W in the central region.

The average number of particles per clan, $\bar{n}_c$, is close to constant at 540 GeV ($\bar{n}_c \simeq 1.75$) over the whole range $-3 < y_1 < +3$. For π^+p (and also pp) at 22 GeV, it has a broad maximum in the centre ($\bar{n}_c \simeq 1.3$). In μp we have again the appearance of a forward--backward asymmetry, at least for $W = 18 \div 20$ GeV: the maximum of $\bar{n}_c$ is reached at $y_1 \simeq -1$ ($\bar{n}_c \simeq 1.2$), whereas $\bar{n}_c \simeq 1.0$ (i.e., a Poissonian MD) at $y_1 \simeq 1$. The clan size in μp coincides with that of π^+p in the backward region $y_1 \lesssim -1$, but is smaller in the central and forward regions, which confirms again the trend noted earlier.

Finally, we can use the μp data on moving windows to test an additivity property mentioned at the end of the Appendix, Eq. (A.27). A sample of results for $W = 18 \div 20$ GeV is given in the Table. Similar tests have been performed for π^+p at 22 GeV and can be found in Ref. [9]. They show that the additivity property only holds for small rapidity windows; it is therefore only for such windows that the data could satisfy the rather extreme assumption of NB behaviour mentioned in the last paragraph of the Appendix.

4. Negative binomial and clan structure in nuclear target experiments

A negative binomial behaviour of MDs has been found also in experiments on proton--nucleus collisions [5], leading again to an analysis in terms of clans. The parameters $\bar{N}$ and $\bar{n}_c$ for rapidity windows $0 < \pm y < y_0$ on Argon and Xenon targets are shown in Figs. 5 and 6, the rapidity being defined in the proton-nucleon c.m. system (NB fits for symmetric windows $\lvert y \rvert < y_0$ were found to be good only for $y_0 \lesssim 2$ when all charged particles are considered; they remain good throughout for negatives). For comparison, proton-proton data folded in one hemisphere are also shown in the figures.

In Fig. 5 the mean number of clans $\bar{N}$ is seen to increase with the atomic number of

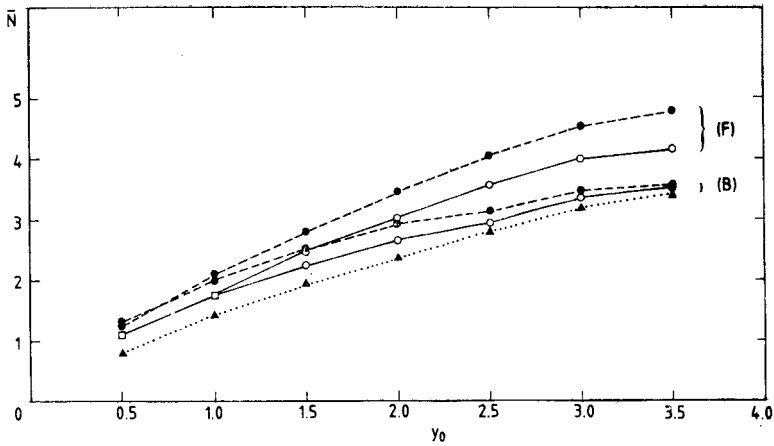

Fig. 5. $\bar{N}$ in proton-nucleus collisions: ○—○ p Ar and ●---● p Xe in rapidity windows $0 < y < y_0$ (F) and $-y_0 < y < 0$ (B), ▲···▲ pp in the same windows folded in one hemisphere. The proton laboratory momentum in 200 GeV/c. The symbol □ indicates the overlap of points

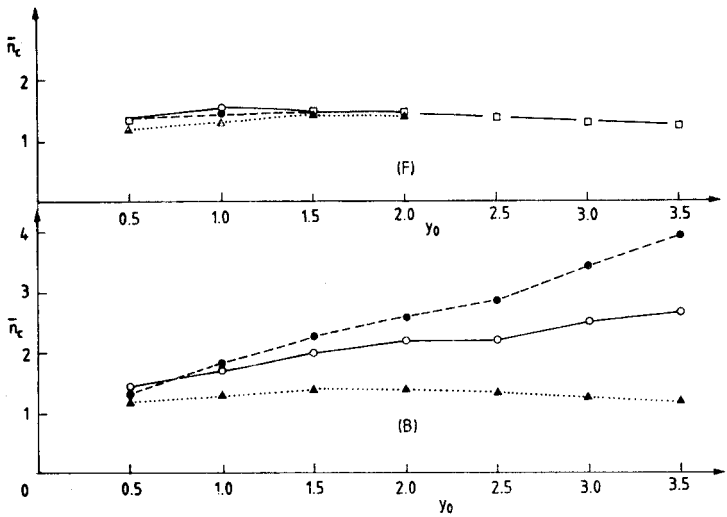

Fig. 6. $\bar{n}_c$ in proton-nucleus collisions. Same notation as in Fig. 4 but the values for $0 < y < y_0$ (F) and $-y_0 < y < 0$ (B) are plotted separately

the target nucleus in both hemispheres, but for large y_0 this A dependence is much stronger in the FH. At $y_0 = 3.5$, for instance, one finds in FH: $\bar{N}(\mathrm{Xe}) \simeq 4.8$, $\bar{N}(\mathrm{Ar}) \simeq 4.2$, $\bar{N}(\mathrm{p}) \simeq 3.4$, to be compared with BH: $\bar{N}(\mathrm{Xe}) \simeq 3.6$, $\bar{N}(\mathrm{Ar}) \simeq 3.5$. In contrast with $\bar{N}$, the clan size parameter $\bar{n}_c$ in FH is practically target-independent and varies little with y_0 (Fig. 6): $\bar{n}_c \simeq 1.5$ for $y_0 \simeq 1.5 \div 2.0$, then slowly decreasing to $\simeq 1.25$. The situation is completely different in BH where $\bar{n}_c$ for $y_0 \lesssim 1$ is much higher for heavier targets and larger rapidity intervals [for instance at $y_0 \simeq 3.5$: $\bar{n}_c(\mathrm{Xe}) \simeq 3.9$, $\bar{n}_c(\mathrm{Ar}) \simeq 2.2$, $\bar{n}_c(\mathrm{p}) \simeq 1.2$].

These remarkable trends are not yet understood. An attempt was made by Fiałkowski [11] who calculated the mean multiplicity and dispersion in backward rapidity windows

for pAr and pXe, on the basis of the multiple collision model of Ref. [12], with good agreement for $\bar{n}$ and fair agreement for k, but without testing the NB character of the MDs. On the other hand, the CERN oxygen and sulfur beam runs on heavy targets ($p_{\text{lab}} = 200$ GeV/c per nucleon) have given MDs which are clearly not of NB shape but can be reproduced quite well by applying multiple collision theory to standard models of pp collisions [13]. It turns out that the shape of the MD for nucleus-nucleus collisions is mainly controlled by the averaging over impact parameter.

In this respect we draw attention to an interesting calculation by Białas and Muryn for MDs of ^{16}O-heavy nucleus collisions at $p_{\text{lab}} = 200$ GeV/c, on the basis of the wounded nucleon model [14]. For central collisions (impact parameter $b = 0$) and a rapidity window $|y| < 0.5$, they find excellent NB fits, with the clan size $\bar{n}_c$ largely independent of the target nucleus (Table I of Ref. [14]). This suggests that in nucleus-nucleus experiments, one should measure the MDs in various rapidity windows, especially in small windows, for events selected by central collision triggers.

Finally, at much lower energy, Cugnon has proposed interesting searches of NB behaviour and clan structure in intranuclear cascade models [15]. In Ref. [15b], a successful test was performed for antiproton annihilation in emulsions at $p_{\text{lab}} = 0 \div 1.4$ GeV/c. The experimental MDs of charged prongs are shown to have NB properties. The theoretical interpretation identifies the ancestors of the clans with the pions coming from the annihilation on a single nucleon, and the clans turn out to have a size independent of the antiproton momentum.

5. NB properties at partonic level

In a very interesting contribution to a recent conference on future accelerators [16], W. Kittel studied the behaviour of e^+e^- annihilation at $\sqrt{s} = 29$, 200 and 2000 GeV as predicted by a Monte Carlo model for coherent parton branching with hadronization by Lund string fragmentation. At 29 GeV the model agrees reasonably well with the data of the HRS Collaboration [2].

At the three energies, the Monte Carlo MDs for charged hadrons in symmetric rapidity windows $|y| < y_0$ are generally close to NB shape, (for large y_0 this holds only for even multiplicities). At fixed $\sqrt{s}$, $\bar{N}$ grows almost linearly with y_0 whereas $\bar{n}_c$ goes through a maximum and then decreases. At fixed y_0, $\bar{n}_c$ grows rapidly with $\sqrt{s}$ whereas $\bar{N}$ is almost constant. Qualitatively, this behaviour is strikingly similar to that observed for the hadronic reactions of Fig. 1, except that the decrease of $\bar{n}_c$ at large y_0 is much stronger.

In these "Monte Carlo experiments", Kittel also examined the MD of all gluons present at the end of the parton cascade when the hadronization sets in. It was found to have NB shape at $\sqrt{s} = 2$ TeV but not at lower energy.

Stimulated by Kittel's results and by the success of the coherent Lund shower model in its most recent version for the description of e^+e^- annihilation data[2], we have used this

[2] The Lund shower model is similar to the Marchesini-Webber model as far as the partonic shower is concerned, but different in the hadronization mechanism which is of string fragmentation type. The most recent version is JETSET 6.3 [17].

version in collaboration with T. Sjöstrand to generate multiplicity distributions of partons and of charged hadrons for quark-antiquark and gluon-gluon systems at $\sqrt{s}$ ranging from 22 GeV to 2 TeV [18]. We find that both classes of MDs, in full phase space and in central rapidity windows, have NB properties analogous to those observed in the hadronic experiments of Fig. 1, again with a stronger decrease of $\bar{n}_c$ at large y_0. We also find a simple relation between the partonic and hadronic distributions, which we link with the concepts of preconfinement and local parton-hadron duality. At partonic level, the results suggest a simple interpretation of the clans as "bremsstrahlung gluon jets" with a geometric MD, which is the simplest type of MD reproducing itself by branching, see Appendix, especially Eqs (A.18) and (A.24). It is by averaging over these geometric clans that the logarithmic MD of an average clan is generated, see Eqs. (A.22) and (A.23). We are therefore led to a simple physical picture of the clan structure at partonic level which carries over to the hadronic level by local parton-hadron duality, and it is natural to conjecture that a similar picture may also hold for hadronic and semi-leptonic processes.

6. Summary and concluding remarks

The main purpose of this paper was to review the negative binomial (NB) properties which have recently been found for many experimental multiplicity distributions of high energy reactions in selected rapidity windows. For this review, instead of characterizing the NB distributions by the usual parameters $\bar{n}$ and k, we have used the parameters $\overline{N}$ and $\bar{n}_c$ attached to the clan structure which is defined mathematically for any NB. The experimental values of $\overline{N}$ and $\bar{n}_c$ turn out to have a series of remarkable properties which can be read directly from the figures of the paper, for instance

(*i*) the high degree of energy independence of the average number of clans, $\overline{N}$, for hadronic reactions in the wide c.m. energy range $\sqrt{s} = 22 \div 900$ GeV (Fig. 1b);

(*ii*) the similarities and differences between hadronic and semi-leptonic reactions (π^+p at $\sqrt{s} = 22$ GeV, μp at hadronic energies $W = 18 \div 20$ GeV) for $\overline{N}$ and the average charged multiplicity per clan, $\bar{n}_c$ (Figs. 2–4);

(*iii*) the dependence of the clan parameters on atomic number in proton-nucleus collisions in the forward and backward hemispheres of the proton-nucleon c.m. system (Figs. 5, 6), especially the contrast between the forward (F) and backward (B) dependence of the clan size on target nucleus (Fig. 6).

These findings led us to the conjecture that the clan structure analysis is more than a mathematical parametrization of the data and should have dynamical relevance. Further support for this view is provided by our recent work on the multiplicity distributions predicted by the Lund Shower Model for e^+e^- annihilation (see Section 5 and Ref. [18]). It suggests a simple interpretation of the clans at partonic level, which carries over to the hadronic level by local parton-hadron duality, and it may lead to progress on the unresolved problem of finding the dynamical explanation for the wide prevalence of NB behaviour in hadronic, semi-leptonic and leptonic reactions.

On the experimental side, the NB properties already provide simple and powerful ways of extrapolating measured multiplicity distributions to the higher energies which will

become available at future e^+e^-, ep and pp colliders. When these machines will operate, the clan analysis and the comparisons between reactions which we have carried out will become possible even with multiplicity data in limited phase space regions. This will apply in particular to the e^+e^- colliders SLC and LEP and to the ep collider HERA, which should make it possible to explore e^+e^- annihilation and semi-leptonic reactions to sufficiently high energies for putting on a firm basis the comparison we made in Sections 2 and 3.

We are indebted to the members of the Collaborations listed in Refs. [1] to [5] for providing us with many data in a form suitable for our analysis, and in particular to I. Derado, M. Derrick, G. Ekspong, W. Kittel, P. Malecki, S. Maselli, F. Meijers and N. Schmitz for help and discussions.

APPENDIX

This appendix groups a number of mathematical properties of the negative binomial multiplicity distribution (NBMD). The NBMD has been defined by using different two-parameter sets. They are of course not independent but to examine each of them separately turns out to be very useful in order to elucidate some of the main properties of the distribution.

The parameters k, $\bar{n}$. The standard way to parametrize the NBMD in multiparticle dynamics has been in terms of the average multiplicity $\bar{n}$ and the positive parameter k, which is related to the dispersion $D = \sqrt{(\overline{n^2} - \bar{n}^2)}$ by

$$\frac{D^2}{\bar{n}^2} = \frac{1}{\bar{n}} + \frac{1}{k}. \tag{A.1}$$

This relation implies that the NBMD is broader than the Poissonian for which $D^2 = \bar{n}$. With these parameters the NBMD has the following form

$$P_0(\bar{n}, k) = \left(\frac{k}{\bar{n}+k}\right)^k, \quad P_n(\bar{n}, k) = P_0(\bar{n}, k) \frac{k(k+1) \ldots (k+n-1)}{n!} \left(\frac{\bar{n}}{\bar{n}+k}\right)^n. \tag{A.2}$$

The corresponding generating function (g.f.) is given by

$$G_{\mathrm{NB}}(\bar{n}, k; z) \equiv \sum_{n=0}^{\infty} z^n P_n(\bar{n}, k) = \left[1 - \frac{\bar{n}}{k}(z-1)\right]^{-k} \tag{A.3}$$

the normalization condition being $G_{\mathrm{NB}}(\bar{n}, k; 1) = 1$. If k is replaced by a negative integer, $-K$, (A.2) transforms into the familiar (positive) binomial MD for $n = 0, \ldots, K$ and $P_n = 0$ for $n > K$. For k negative non-integer, (A.2) is not a probability distribution.

The parameters a, b and the recurrence relation. A necessary and sufficient condition for a multiplicity distribution (MD) P_n to be a NBMD is the recurrence relation

$$\frac{(n+1)P_{n+1}}{P_n} = a + bn; \quad n = 0, 1, \ldots, \tag{A.4}$$

where a, b are positive constants and $b < 1$. It can easily be seen that (A.2) satisfies the relation (A.4) with

$$a = \frac{\bar{n}k}{\bar{n}+k}, \qquad b = \frac{\bar{n}}{\bar{n}+k}. \tag{A.5}$$

Conversely, iteration of (A.4) gives

$$P_n = P_0 a(a+b) \ldots [a+b(n-1)]/n!, \qquad P_0 = (1-b)^{a/b} \tag{A.6}$$

with P_0 obtained by normalization. This is equivalent to (A.2) with the relations (A.5). In terms of a and b, the g.f. (A.3) is

$$G_{\mathrm{NB}}(\bar{n}, k; z) = \left(\frac{1-b}{1-bz}\right)^{a/b}. \tag{A.7}$$

We mention two limiting cases:

I. In the limit $b \to 0$ (i.e., $k \to \infty$ and $a \to \bar{n}$), the recurrence relation shows immediately that the NBMD reduces to a Poisson distribution

$$P_{\mathrm{P}}(n) = P_{\mathrm{P}}(0)a^n/n!, \qquad a = \bar{n}, \qquad P_{\mathrm{P}}(0) = e^{-a}. \tag{A.8}$$

The value of $P_{\mathrm{P}}(0)$ is given by normalization. The g.f. (A.7) becomes

$$G_{\mathrm{P}}(\bar{n}; z) = e^{\bar{n}(z-1)}. \tag{A.9}$$

II. The limiting case $a \to 0$ at constant b is also interesting, but one must truncate the NBMD to $n \geqslant 1$ because $P_0 \to 1$ in (A.6). Solving the recurrence relation for $n \geqslant 1$ now gives the logarithmic MD

$$P_{\mathrm{l}}(n) = P_{\mathrm{l}}(1)b^{n-1}/n, \qquad n > 1; \qquad P_{\mathrm{l}}(1) = -b/\ln(1-b), \tag{A.10}$$

$P_{\mathrm{l}}(1)$ is obtained by normalization. The average multiplicity is

$$\bar{n}_{\mathrm{l}} = \frac{-b}{(1-b)\ln(1-b)} \tag{A.11}$$

and the g.f.

$$G_{\mathrm{l}}(b; z) = \frac{\ln(1-bz)}{\ln(1-b)}. \tag{A.12}$$

For $a > 0$, $b < 0$ and a/b integer the recurrence relation gives the positive binomial MD.

The parameters $\bar{n}_c$ and $\bar{N}$ and the clan structure. The NBMD can be obtained as a composition of Poisson and logarithmic MDs. We are interested in this approach for two reasons: (*i*) it leads to the concept of "clan" for which remarkable properties are found from the data; (*ii*) it shows that the NBMD belongs to a more general class of MD, which are known in the statistical literature as infinitely divisible (ID) or compound Poisson distributions. Every NBMD can be generated by independent emission of groups of particles which we

call clans[3] and which have on the average a logarithmic MD. The number N of clans has a Poisson distribution with average $\bar{N}$. The simplest proof of this property is in terms of the g.fs. (A.7), (A.9) and (A.12)

$$G_{\mathrm{NB}}(\bar{n}, k; z) = G_{\mathrm{P}}(\bar{N}; G_{\mathrm{l}}(b; z)) \tag{A.13}$$

a relation which holds if

$$\bar{N} = -\frac{a}{b}\ln(1-b) = k\ln\left(1+\frac{\bar{n}}{k}\right). \tag{A.14}$$

In our definition every clan contains at least one particle, corresponding to $G_{\mathrm{l}}(b, 0) = 0$. The average number of particles in a clan, which we usually denote by $\bar{n}_{\mathrm{c}}$, is given by (A.11). As is easily verified, (A.11) and (A.14) give

$$\bar{n}_{\mathrm{c}} \equiv \bar{n}_1 = \bar{n}/\bar{N}.$$

For a Poisson distribution ($k \to \infty$, $b \to 0$), $P_{\mathrm{l}}(n)$ of (A.10) reduces to δ_{n1} and the clans are composed of a single particle, so that $\bar{N} = \bar{n}$, $\bar{n}_{\mathrm{c}} = 1$. When a NBMD is close to Poisson, the error on k gets large and the parameter set (a, b) becomes inconvenient ($a \simeq 1$, $b \simeq 0$). The sets $(\bar{n}, k^{-1})$ and $(\bar{n}_{\mathrm{c}}, \bar{N})$ are then more appropriate. On the other hand, for a positive binomial, the clan structure loses its meaning because $b < 0$ and the quantities (A.10) are negative for even n.

Infinitely divisible (ID) distributions. The ID distributions are the MDs obtained by independent emission of groups of particles ("clans") which have an arbitrary MD. Their g.f. $G_{\mathrm{ID}}(\bar{N}; z)$ is given by replacing in (A.13) the logarithmic g.f. G_{l} by an arbitrary g.f. $G(z)$:

$$G_{\mathrm{ID}}(\bar{N}; z) = G_{\mathrm{P}}(\bar{N}; G(z)). \tag{A.15}$$

The number N of clans still has a Poisson distribution (hence the name "compound Poisson") but the MD of the clans is now given on the average by the g.f. $G(z)$. The name ID expresses the property that for any integer $L > 0$, the MD of g.f. (A.15) is the convolution of L identical MDs. This follows immediately from (A.15) by noting that

$$G_{\mathrm{ID}}(\bar{N}; z) = \{G_{\mathrm{P}}[\bar{N}/L; G(z)]\}^L. \tag{A.16}$$

It can be shown that the converse also holds: if a MD is the convolution of L identical MDs for every L, its g.f. is of the form (A.15) with $G(z)$ a g.f., i.e., $G(z) = \Sigma p_n z^n$ and $p_n \geqslant 0$ for all n[4]. This $G(z)$ is unique if one adopts the convention $p_0 = 0$ (every clan has at least one particle).

---

[3] In Ref. [7a] a "clan" was called "cluster". In Ref. [7b], the name is changed to avoid confusion with the cluster concept commonly used to describe short-range two-particle correlations. The word clan refers to the fact that, in simple cascade models producing NBMDs, the clans are groups of particles of common ancestry.

[4] This can be deduced from the Lévy-Khinchine "canonical representation" [theorem 5.5(1) p. 117, in E. Lukacs, *Characteristic Functions*, 2nd Edition, Griffin, London 1970] by specializing to the case of a probability distribution over non-negative integers.

Cugnon and Harouna [19] have recently shown that a distribution of g.f. (A.15) remains close to NB shape even when the MD of g.f. $G(z)$ departs considerably from the logarithmic form (A.12).

The relation of the NBMD to the geometric distribution. It is interesting that several properties of a NBMD can be concisely expressed in terms of the differential of the g.f. G_{NB}. This is best done by choosing z, k and the ratio $\bar{n}/k$ (or equivalently b) as three independent variables. Starting from (A.7) and using $a = kb$ from (A.5), an elementary calculation gives

$$d \ln G_{NB} = \frac{adz}{1-bz} + \ln G_{NB} \frac{dk}{k} + k[G_g(\nu; z)-1] \frac{d\nu}{\nu} \tag{A.17}$$

with

$$\nu = (1-b)^{-1} = 1 + \frac{\bar{n}}{k}, \quad G_g(\nu; z) = \frac{z}{\nu + z - \nu z} \tag{A.18}$$

G_g is the g.f. of the (truncated) geometric MD with probabilities

$$P_g(0) = 0, \quad P_g(n) = (\nu-1)^{n-1}/\nu^n, \quad n = 1, 2, \ldots \tag{A.19}$$

ν is its average multiplicity.

If we apply (A.17) at constant k and b, we obtain

$$(1-bz) \frac{\partial}{\partial z} G_{NB} = aG_{NB}. \tag{A.20}$$

With (A.3), this is equivalent to the recurrence relation (A.4). Secondly, applying (A.17) at constant z and b, we obtain that $\ln G_{NB}$ is proportional to k:

$$\ln G_{NB}(\bar{n}, k; z) = k \ln G_{NB}\left(\frac{\bar{n}}{k}, 1; z\right), \tag{A.21}$$

which implies the infinite divisibility of the NBMD. Thirdly, (A.17) taken at constant z and k can be integrated over $1 \leqslant \nu' \leqslant \nu$ to give

$$\ln G_{NB} = k \int_1^{\nu} [G_g(\nu'; z)-1] \frac{d\nu'}{\nu'} \tag{A.22}$$

(remember that $G_{NB} = 1$ for $b = 0$). This is directly related to the clan structure expressed by (A.13) because one verifies with (A.12), (A.14) and (A.18)

$$\bar{N} = k \ln \nu, \quad G_1(b; z) = \left[\int_1^{\nu} G_g(\nu'; z) \frac{d\nu'}{\nu'}\right] \Big/ \ln \nu. \tag{A.23}$$

The natural interpretation is to regard the average clan with its logarithmic MD as an average over geometric clans. In other words, the NBMD is generated by independent emission of geometric clans with mean multiplicity v' in the interval $(1, v = 1+\bar{n}/k)$, the average number of geometric clans in $(v', v'+dv')$ being kdv'/v'.

The geometric MD obeys the differential equation

$$v\frac{\partial}{\partial v}G_g(v; z) = G_g(v; z)\,[G_g(v; z)-1]. \tag{A.24}$$

Expressed in terms of the probabilities $P_g(n)$ of (A.19), this relation describes the simplest form of self-similar branching process. It was encountered by one of the present authors in the Markov process version [20] of the Konishi-Ukawa-Veneziano QCD jet calculus [21] when applied to gluons in absence of quarks.

The NB parameter k^{-1} as a measure of aggregation. As shown in the Appendix of Ref. [7b], one easily proves that for a NBMD the probability $P_N(n)$ to have n particles belonging to N clans obeys the recurrence relation

$$P_N(n)/P_{N+1}(n) = k^{-1}d_N(n)/d_{N+1}(n), \tag{A.25}$$

where

$$d_N(n) = (n!/N!)\Sigma^*(n_1 \ldots n_N)^{-1}.$$

The sum Σ^* runs over all partitions $n = n_1 + \ldots n_N$ with the n_i integers $\geqslant 1$. For example

$$P_1(2)/P_2(2) = k^{-1}.$$

The relation (A.25) does not depend on the mean multiplicity $\bar{n}$. It shows that k^{-1} can be regarded as an *aggregation coefficient* between clans.

NBMD in continuous domains. One of the present authors [22] studied the class of distributions of points in a continuous domain D_0, characterized by the rather extreme assumption that the multiplicity of points *in D_0 and in every connected or disconnected subdomain D* of D_0 has a NB distribution. He showed that a distribution of this class is completely determined by the two functions $Q_1(y) = d\bar{n}/dy$ and $k(y)$, where $d\bar{n}$ and $k(y)$ are the average multiplicity and k-parameter of the NBMD in the infinitesimal neighbourhood dy of the point y. For a general subdomain D, the NB parameters $\bar{n}_D$ and k_D are given by

$$\bar{n}_D = \int_D dyQ_1(y), \qquad \bar{n}_D/k_D = \int_D dyQ_1(y)/k(y). \tag{A.26}$$

For non-overlapping domains D_i and their union D, Eqs. (A.26) give the additivity property

$$\Sigma\,(\bar{n}_{D_i}/k_{D_i}) = (\Sigma\,\bar{n}_{D_i})/k_D = \bar{n}_D/k_D. \tag{A.27}$$

REFERENCES

[1] G. J. Alner et al. (UA5 Collaboration), *Phys. Lett.* **B160**, 199 (1985); *Phys. Lett.* **B160**, 193 (1985); *Phys. Lett.* **B167**, 47 (1986).

[2] M. Derrick et al. (HRS Collaboration), *Phys. Lett.* **B168**, 299 (1986); *Phys. Rev.* **D34**, 3304 (1986).

[3] M. Adamus et al. (NA22 Collaboration), *Phys. Lett.* **B177**, 239 (1986); *Z. Phys.* **C32**, 475 (1986).

[4] M. Arneodo et al. (EMC), *Z. Phys.* **C35**, 335 (1987).

[5] F. Dengler et al. (NA5 Experiment), *Z. Phys.* **C33**, 187 (1986).

[6] G. Giacomelli, *Inclusive and semi-inclusive hadron interactions at ISR energies*, invited paper at Les Rencontres de Physique de la Vallé d'Aoste, La Thuile, Italy, Bologna preprint DFUB 87/13 (1987).

[7] a) A. Giovannini, L. Van Hove, *Z. Phys.* **C30**, 213 (1986); b) L. Van Hove, A. Giovannini, in Proceedings of XVII International Symposium on Multiparticle Dynamics, ed. M. Markytan et al., World Scientific, Singapore 1987, p. 561.

[8] G. J. Alner et al. (UA5 Collaboration), CERN EP/85-61, Table 4, 2nd column.

[9] M. Adamus et al. (EHS/NA22 Collaboration), *Phase space dependence of the multiplicity distribution in π^+p and pp collisions at 250 GeV/c*, Nijmegen preprint HEN-284 (1987).

[10] M. Arneodo et al. (EMC), *Z. Phys.* **C35**, 335 (1987), and private communication from S. Maselli (EMC-NA9 Collaboration, paper in preparation).

[11] K. Fiałkowski, *Phys. Lett.* **B191**, 191 (1987).

[12] E. Błeszyńska, M. Błeszyński, W. Czyż, *Acta Phys. Pol.* **B8**, 393 (1977).

[13] First results were presented at the 6th International Conference on Ultra-Relativistic Nucleus-Nucleus Collisions (Quark Matter 87), Nordkirchen, FR Germany, 24–28 August 1987. See the Proceedings, ed. H. Satz et al., Z. Phys. C. to appear.

[14] A. Białas, B. Muryn, *Acta Phys. Pol.* **B18**, 51 (1987); For the wounded nucleon model, see: A. Białas, M. Błaszyński, W. Czyż, *Nucl. Phys.* **B111**, 461 (1976).

[15] a) J. Cugnon, *Z. Phys.* **A237**, 187 (1987); b) J. Cugnon, P. Jasselette, J. Vandermeulen, *Europhys. Lett.* **4**, 535 (1987).

[16] W. Kittel, in Proceedings of the Workshop on Physics at Future Accelerators, La Thuile and Geneva 1987, CERN Report 87–07, Vol. II, p. 424.

[17] M. Bengtsson, T. Sjöstrand, *Nucl. Phys.* **B289**, 810 (1987); T. Sjöstrand, M. Bengtsson, *Comput. Phys. Commun.* **43**, 367 (1987), esp. section (6.3), The coherent evolution case. For a comparison with experiments: A. Petersen et al., *Phys. Rev.* **D37**, 1 (1987).

[18] L. Van Hove, A. Giovannini, *Multiplicity distributions in the Lund Shower Model of e^+e^- annihilation*, CERN preprint TH. 4885/87 (1987).

[19] J. Cugnon, O. Harouna, *Europhys. Lett.* **4**, 1127 (1987).

[20] A. Giovannini, *Nucl. Phys.* **B161**, (1979) 429.

[21] K. Konishi, A. Ukawa, G. Veneziano, *Nucl. Phys.* **B157**, 45 (1979).

[22] L. Van Hove, *Physica* **147A**, 19 (1987),